



저작자표시-비영리-변경금지 2.0 대한민국

이용자는 아래의 조건을 따르는 경우에 한하여 자유롭게

- 이 저작물을 복제, 배포, 전송, 전시, 공연 및 방송할 수 있습니다.

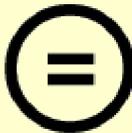
다음과 같은 조건을 따라야 합니다:



저작자표시. 귀하는 원저작자를 표시하여야 합니다.



비영리. 귀하는 이 저작물을 영리 목적으로 이용할 수 없습니다.



변경금지. 귀하는 이 저작물을 개작, 변형 또는 가공할 수 없습니다.

- 귀하는, 이 저작물의 재이용이나 배포의 경우, 이 저작물에 적용된 이용허락조건을 명확하게 나타내어야 합니다.
- 저작권자로부터 별도의 허가를 받으면 이러한 조건들은 적용되지 않습니다.

저작권법에 따른 이용자의 권리는 위의 내용에 의하여 영향을 받지 않습니다.

이것은 [이용허락규약\(Legal Code\)](#)을 이해하기 쉽게 요약한 것입니다.

[Disclaimer](#)

Master's Thesis

Practical Partial Row Activation  
for 3D Stacked DRAM with  
Applications to Deep Learning  
Workloads

3D 적층 DRAM을 위한 실용적인 Partial Row  
Activation 및 딥 러닝 워크로드에의 적용

February 2019

Graduate School of Seoul National University  
Computer Science and Engineering

Namho Kim

# Practical Partial Row Activation for 3D Stacked DRAM with Applications to Deep Learning Workloads

3D 적층 DRAM을 위한 실용적인 Partial Row  
Activation 및 딥 러닝 워크로드에의 적용

Advisor Jae W. Lee

Submitting a master's thesis of engineering

January 2019

Graduate School of Seoul National University

Computer Science and Engineering

Namho Kim

Confirming the master's thesis written by Namho Kim

January 2019

Chair Jihong Kim (Seal)

Vice Chair Jae W. Lee (Seal)

Examiner Jaejin Lee (Seal)

## Abstract

# Practical Partial Row Activation for 3D Stacked DRAM with Applications to Deep Learning Workloads

Namho Kim

Department of Computer Science and Engineering

The Graduate School

Seoul National University

GPUs are widely used to run deep learning applications. Today’s high-end GPUs adopt 3D stacked DRAM technologies like High-Bandwidth Memory (HBM) to provide massive bandwidth, which consumes lots of power. Thousands of concurrent threads on GPU cause frequent row buffer conflicts to waste a significant amount of DRAM energy. To reduce this waste we propose a *practical* partial row activation scheme for 3D stacked DRAM. Exploiting the latency tolerance of deep learning workloads with abundant memory-level parallelism, we trade DRAM latency for energy savings. The proposed design demonstrates substantial savings of DRAM activation energy with minimal performance degradation for both the deep learning and other conventional GPU workloads. This benefit comes with a very low area cost and only minimal adjustments of DRAM timing parameters to the standard HBM2 DRAM interface.

**Keywords:** DRAM Architecture, GPU, Convolutional Neural Network, HBM2,

Power Efficiency

**Student Number:** 2017-22393

# Contents

<b>Abstract</b>	<b>i</b>
<b>Contents</b>	<b>iv</b>
<b>Chapter 1 Introduction</b>	<b>1</b>
<b>Chapter 2 Background and Motivation</b>	<b>4</b>
2.1 Deep Learning Workloads . . . . .	4
2.2 DRAM Access Patterns on GPU . . . . .	7
2.3 Partial Row Activation . . . . .	9
2.4 Performance/Area Trade-off in Partial Activation . . . . .	10
2.5 Latency-Tolerance of Deep Learning Workloads on GPU . . . . .	11
<b>Chapter 3 Practical Partial Row Activation</b>	<b>13</b>
3.1 Overview . . . . .	13
3.2 Bank Structure . . . . .	13
3.3 Delayed Activation . . . . .	17
<b>Chapter 4 Evaluation</b>	<b>19</b>
4.1 Methodology . . . . .	19
4.2 DRAM Energy Savings . . . . .	21
4.3 Performance Impact . . . . .	22
4.4 Area Overhead . . . . .	24

Chapter 5 Conclusion	25
Bibliography	26
국문초록	30
Acknowledgements	31

# List of Tables

Table 4.1	Platform parameters . . . . .	20
Table 4.2	DRAM system parameters . . . . .	20
Table 4.3	HBM2 timing parameters . . . . .	20

# List of Figures

Figure 2.1	FC and CONV layer algorithms . . . . .	5
Figure 2.2	Convolution structure and computation methodology . .	6
Figure 2.3	DRAM access patterns executing cuda-convnet on each layer . . . . .	8
Figure 2.4	Performance degradation with longer column latency ( $\tau_{AA}$ )	11
Figure 3.1	Baseline HBM2 architecture . . . . .	14
Figure 3.2	Detailed view of PPA bank architecture . . . . .	15
Figure 3.3	Data fetch timing diagram through the narrow bitline . .	16
Figure 3.4	Waveform of proposed delayed activation . . . . .	17
Figure 4.1	Activation energy savings on CNN and MLP workloads .	21
Figure 4.2	Activation energy savings on general workloads (Rodinia and STREAM) . . . . .	21
Figure 4.3	DRAM energy savings on CNN and MLP workloads . .	22
Figure 4.4	DRAM energy savings on general workloads (Rodinia and STREAM) . . . . .	22
Figure 4.5	Performance degradation on CNN and MLP workloads .	23
Figure 4.6	Performance degradation on general workloads (Rodinia and STREAM) . . . . .	23

# Chapter 1

## Introduction

The recent advent of throughput computing with Graphics Processing Units (GPU) led an increase in demand for the memory bandwidth. To meet this increasing demand for memory bandwidth, 3D-stacked memory technologies such as High-Bandwidth Memory (HBM) [1] or Hybrid Memory Cube [2] have been proposed and now widely used in production GPUs and general-purpose processors. While these recent advances in memory system help throughput-oriented computing devices to exploit higher level of parallelism, this trend of increased memory bandwidth is also increasing the amount of power/energy spent on the memory system. For example, a future HBM-based memory system providing 4TB/s memory bandwidth for GPU is expected to use over 150W power [3].

One of the primary components in DRAM energy consumption is the *row access energy* which is consumed when a DRAM row is activated (i.e., latch data of a DRAM row into the row buffer) and precharged (i.e., restore the bitline voltage). One main issue here is that the size of row is often much larger than the minimum amount of data that a GPU needs. For example, in HBM2 (with pseudo-channel mode [1]), the size of DRAM row is 1KB while the last level cacheline size of a GPU is often 128 bytes. This is not really a problem if there are many column accesses happening while the row is open. However, with a

huge amount of parallelism provided by GPUs, a row is likely to close before several column accesses happen [3, 4]. As a result, the amount of energy spent on row accesses remains a substantial component of DRAM energy consumption.

To address this problem, partial row activation schemes [3, 4, 5, 6] have been proposed, which only activate part of the row that is likely to be accessed. By doing so, these proposals can avoid the problem of row over-fetching and reduce the amount of energy spent on row accesses. However, many of these proposals often incur significant area overhead reported to be 12% to 34% [5, 6], which negatively affects both yield and capacity of DRAM. More importantly, most previous proposals require substantial changes to the standardized memory controller interface (e.g., JEDEC standard). While such changes may enable higher performance gains or energy savings, adopting such changes to a real system requires a significant amount of effort from multiple stakeholders, such as memory vendors, processor vendors, and memory standardization committee. Instead, we advocate more *localized* solutions with minimal extensions to the existing memory interface for easy deployment.

Thus, we present a *practical* partial row activation scheme which neither incurs noticeable area overhead nor requires any modification to the memory interface or controller. Exploiting the fact that many emerging GPU workloads, such as deep neural networks, are latency-tolerant by nature, we propose a partial row activation scheme requiring only minimal changes in DRAM and thus can be used as a drop-in replacement for existing, real HBM2 systems. The proposed ready-to-deploy scheme substantially reduces the amount of energy spent on row accesses at the expense of negligible performance degradation in most GPU workloads.

The rest of this thesis is organized as follows. Chapter 2 describes the features of deep learning workload and its DRAM access pattern on GPU and

motivates this work. Chapter 3 elaborates on the proposed practical partial activation scheme which includes the bank structure for partial row activation and its timing. Chapter 4 presents the evaluation methodology and the results. Finally, we conclude the paper in Chapter 5.

## Chapter 2

# Background and Motivation

### 2.1 Deep Learning Workloads

Memory performance is an important factor that affects overall DNN performance, even in domain-specific architectures. For instance, TPU [7] shows that the array active cycle is 78.2% with 86.0 TOPS/sec in CNN. The weight stall cycle is 0% as CNNs reuse it in many domain-specific architectures. However, TPU performance is limited when executing MLP and RNN as they require high memory bandwidth. In MLP and LSTM, the weight stall cycle is 53.9% and 58.1% that fetches from memory. They try increasing memory bandwidth as four times, and the MLP and LSTM performance increase three times. Also, they found that higher memory bandwidth reduces on-chip memory pressure. We take CNNs, which is widely used DNNs, as an example. Most layers in CNNs consist of convolution (CONV) layer and fully connected (FC) layer. Figure 2.1 (a) shows the base algorithm of FC layers, whose computation is general matrix-vector multiplication. The structure of data and weight are usually vector and matrix. Sequential as you see in the code, and it means DRAM access also shows sequential patterns. On the other hand, as shown in Figure 2.1 (b), traditional CNN compute 3D data and 4D weight matrix multiplication.

It takes  $O_c \times O_h \times O_w$  output multiplying  $I_c \times I_h \times I_w$  data with  $O_c \times I_c \times K_h \times K_w$  weight. The convolution filter slides to each input features and accumulates

```

1 // FC layer computation
2 // Stride: 1
3 float output[Oc];
4 float input[Ic][H][W];
5 float weight[Oc][Ic][H][W];
6
7 for(int o=0; o<Oc; ++o){
8   for(int i=0; i<Ic; ++i){
9     for(int h=0; h<H; ++h){
10      for(int w=0; w<W; ++w){
11        output[o]=input[i][h][w]
12          *weight[c][i][h][w];
13      }}}

```

(a) FC layer computation

```

1 // Convolution layer
2 // Stride: 1, pad: 0
3 float output[Oc][H][W];
4 float input[Ic][H][W];
5 float weight[Oc][Ic][K][K];
6
7 // Computation of CONV.
8 for(int o=0; o<Oc; ++o){
9   for(int h=0; h<H; ++h){
10    for(int w=0; w<W; ++w){
11      float sum = 0.f;
12      for(int i=0; i<Ic; ++i){
13        for(int fh=0; fh<K; ++fh){
14          for(int fw=0; fw<K; ++fw){
15            int in_h = h+fh;
16            int in_w = w+fw;
17            sum+=input[i][in_h][in_w]
18              *weight[o][i][fh][fw];
19          }}}
20      output[o][h][w]=sum;
21    }}}

```

(b) CONV layer computation

Figure 2.1: FC and CONV layer algorithms

to make one pixel of output feature. In this computation, one convolution filter may meet an input pixel twice or more. As this character, CNNs have two issue that decreases the GPU performance. First, there is a lot of duplicated data usage when computing convolution kernel parallel. Weight is used for all input data and shared as thread index, but input data gets different thread and block index even though the value is same. Also, GPUs should call lots of kernels computing each convolution as all matrix multiplication is independent. These kernels are called at GPU core randomly and the memory access pattern is hard to predict what data to gather in the cache. Besides, the GPU kernel size is bound to the convolution kernel size. Most CNNs use convolution kernels with the size from  $11 \times 11$  [8] to  $1 \times 1$  [9] to get accurate features using the data. This is significantly small compared to the maximum number of thread, usually 512 or 1024, in the kernel on GPU, and it causes the limitation of parallelism executing overall CNNs. There is another issue when using small convolution

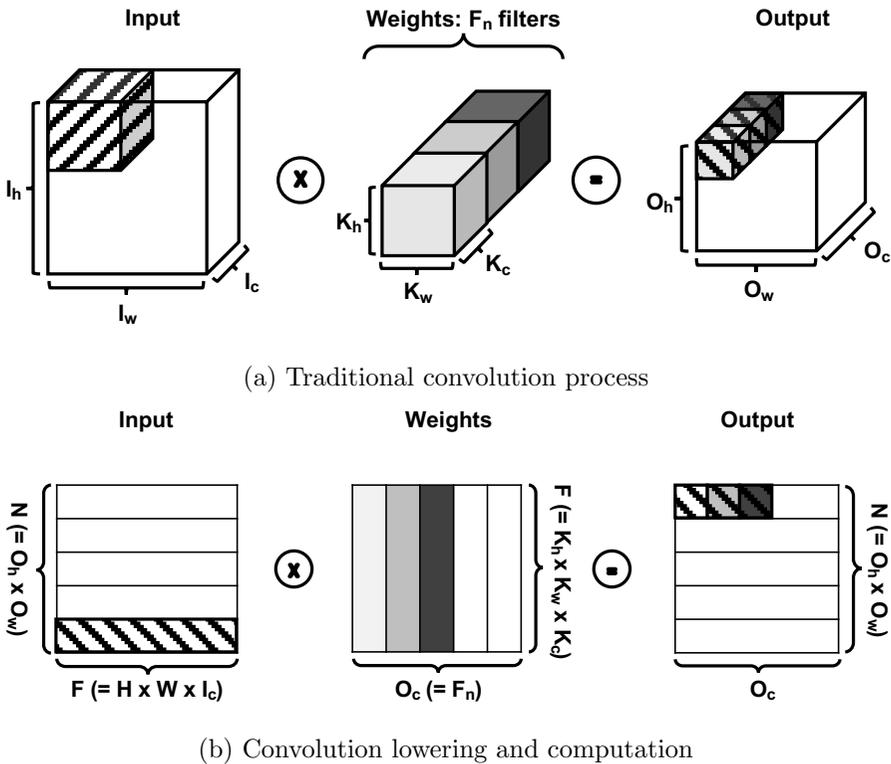


Figure 2.2: Convolution structure and computation methodology

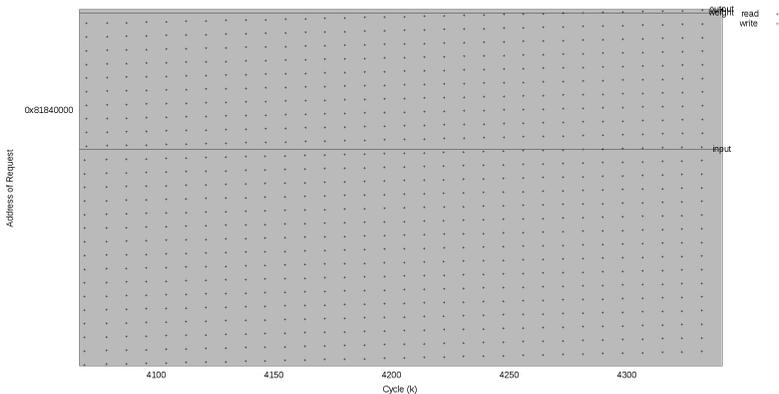
kernels. When it uses general  $3 \times 3$  convolution kernels, boundary check needs to compute the convolution kernel. The condition flow in GPU is processed one-by-one execution and it decreases the GPU performance at least twice. As memory access range is high in CNNs, it shows inefficient memory bandwidth.

To optimize memory bandwidth software transformations like convolutional lowering are performed to access memory sequentially. cuDNN [10] uses `im2col` function to convolutional lowering as depicted in Figure 2.2 (b).  $I_c \times I_h \times I_w$  input data is changed as  $I_c \times K_h \times K_w \times I_h \times I_w$  column. After transforming, the convolution kernel executes general matrix multiplication (GEMM) with column and weight. Though convolution lowering requires the amount of memory area

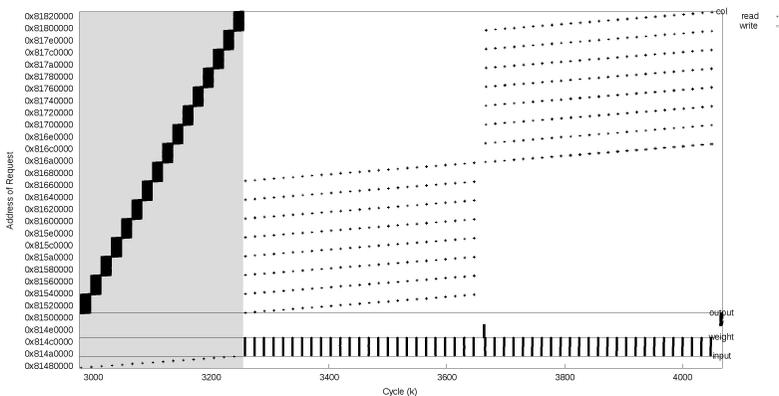
due to saving the transformed matrix, it helps to serialize the GPU kernel and increase memory bandwidth as it does not check the boundary of the kernel and fetches continuous data.

## 2.2 DRAM Access Patterns on GPU

Both CONV (`im2col + GEMM`) and FC layers demonstrate largely sequential memory access patterns, to maximize DRAM bandwidth and minimize over-fetching. Figure 2.3 (a) describes the last FC layer DRAM access patterns. It reads DRAM on the regular step, which is the same as the stride of each data and weight values. The output data is written at DRAM, in general, to pass over it to the next layer. In this example, however, the output number of the last FC layer is only 10 that is small to remain the cache. Also, it reuses directly at `softmax` function, which makes probability vector to prediction. Hence, it does not have to access additional DRAM access to write the output. In contrast, Figure 2.3 (b) is divided into two sides; one for convolution lowering, and the other for matrix multiplication. There are many DRAM write access (`0x81520000 ~ 0x81820000`) because of saving the transformed matrix data in the memory, while few DRAM read access (`0x81480000 ~ 0x814a0000`) to get original input data. It might be possible to transform the data layout of a tensor to maximize row buffer locality. Although this approach has an advantage for deployment on commodity hardware, it is very difficult to implement it as it requires the knowledge of DRAM address mapping. Today's GPUs allocate some of the column address bits to high-order bits (with optional XOR address hashing) to minimize DRAM bank conflicts. This implies that even a simple one-dimensional array is interleaved over multiple banks in a non-contiguous manner. Thus, it is very challenging to optimize the data layout purely in soft-



(a) FC layer



(b) CONV layer

Figure 2.3: DRAM access patterns executing cuda-convnet on each layer

ware. Besides, even if the data layout of a single array is carefully optimized, there are many concurrent thread blocks accessing the array out of order. The state-of-the-art SM scheduler does not take into account DRAM row buffer locality, and its non-deterministic behaviors make DRAM locality optimization in software even more difficult.

## 2.3 Partial Row Activation

Partial row activation scheme is a well-known technique to mitigate the over-fetching problem. Earlier works including Fujitsu Fast Cycle RAM (FCRAM) [11], fine-grained activation DRAM [5] and [6]. These works can attain plenty of activation energy saving. However, that comes with a significant area overhead due to many peripherals (i.e., lower cell efficiency) which support fine-grained activation. Fine-grained activation [5] added a one-hot decoder and a single AND gate to the wordline of each division in a row. The division of row is selected and activated when earning both row and column address. Using Posted-CAS command, DRAM controller sends row and column command back-to-back cycle. It reduced the DRAM power by up to 40%.

Selective bitline activation (SBA) and single subarray access (SSA) [6] fundamentally re-organized the layout of DRAM arrays and the mapping of data to these arrays so that an entire cache line was fetched from a single subarray. Introducing new protocol existing JEDEC DRAM interface called Posted-RAS, which hold the row address until the column address arrives to activate the bitline selectively. It reduced dynamic and background energy about  $5\times$ .

More recent work addresses these problems but requires changes to the DRAM interface and protocols. [3, 4, 12, 13, 14, 15] Many of these proposals make use of memory controller side information when issue column commands (posted-CAS [16]) or introduce new DRAM commands. [12], for example, partial row activation mask is required from the memory controller after row command issued to activate the dirty cache block.

Half-DRAM [13] proposed a reconstructed DRAM architecture to address the row overfetching problem. By splitting one mat into two parts, it enables half row activation which is almost no bandwidth loss while achieving row

activation power saving. As to the extending Half-DRAM which can perform one-eighth row activation, it has a relatively large area overhead.

Fine-grained DRAM and subchannel [3, 4] proposed a new high-bandwidth DRAM architecture to improve bandwidth by four times and energy efficiency by twice compared to existing HBM2 reorganizing HBM2 channel structure into the narrow parallel channel to mitigate latency overhead due to the narrow path of the fine-grained activation structure. But these works require significant modification of microarchitecture of DRAM core that incurs the area overhead up to 10%.

## 2.4 Performance/Area Trade-off in Partial Activation

Many previous studies identify the row access energy as a major component of DRAM dynamic energy [6, 14]. As a result, there are multiple proposals on partial row activation of DRAM. However, as we hinted earlier, most of these works require a substantial area overhead or changes to the DRAM protocol. This is because of a trade-off between cost (area) and performance. In a conventional DRAM architecture, a DRAM row is striped across multiple DRAM cell arrays, or *mats*. Upon an **ACTIVATE** command a whole row of each mat is latched. Then, when a **READ** command arrives, each mat provides the same number of bits (i.e., 16 bits in HBM2 pseudo-channel mode) based on the provided column address from latches and outputs them to the bus. One potential way to enable partial activation is to segment every single row of each mat and activate only part of the selected row within a mat. However, this requires adding a large number of AND gates and local wordlines to incur huge area overhead [6]. Another potential way is to re-arrange DRAM column data layout so that a single mat (or a few mats) contains the whole contents of a column in a row.

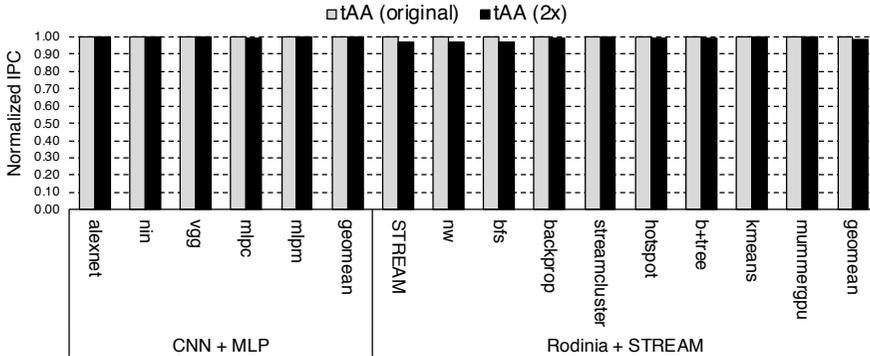


Figure 2.4: Performance degradation with longer column latency ( $t_{AA}$ )

This design can implement partial activation by letting only a single mat to be activated but it incurs a performance overhead as such design needs to output data through a narrow path between a single mat and the I/O, thus incurring serialization delay. An alternative to the previous approach is to increase the width of a path between a single mat and the bus to avoid performance penalty, which also results in a large area overhead.

## 2.5 Latency-Tolerance of Deep Learning Workloads on GPU

One important characteristic of the emerging GPU workloads is that they are tolerant to a long memory latency. Such workloads are often embarrassingly parallel and GPU exploits this characteristic by scheduling multiple warps (e.g., 64) to a single streaming multiprocessor (SM). When a warp in the SM cannot execute due to memory latency, another warp in the SM will be run instead. With this mechanism, the SM can effectively utilize its compute units and operate at a near-perfect efficiency despite the presence of long-latency memory operations. Figure 2.4 demonstrates the latency tolerance of two popular types

of deep learning workloads, convolutional neural networks (CNNs) and multi-layer perceptrons (MLPs), by presenting the performance impact of increasing the  $t_{AA}$  timing parameter (i.e., internal read command to data output) by  $2\times$ . As shown in the figure, all five workloads show no performance degradation. The other conventional GPU workloads also show at most 4% performance degradation. Note that this does not mean that the memory system is not important for GPU workloads. While they are less sensitive to memory latency, most GPU workloads, due to its high degree of parallelism, require large memory bandwidth. Based on this observation, we propose to trade DRAM latency for energy savings in this work.

## Chapter 3

# Practical Partial Row Activation

### 3.1 Overview

The baseline HBM2 device is organized as follows: base and core die slice which is stacked up to 8-Hi slices. The core die slice has 4 channels interconnected by TSV as shown Figure 3.1, Each of which has four quadrants with 16 banks/quadrant. Each quadrant, a channel is assigned 128 TSV I/Os in the TSV area across the core slice. Currently, we assume that our baseline HBM2 device consists of 4-Hi slices. So individual channel has 32 banks divided into upper and lower slice group.

We introduce two terminologies to the baseline HBM2 design: *sectors* and activation bit vector. The *sector* is a minimum activation granularity of row buffer. We divide row buffer into 8 *sectors* from previous partial activation schemes from [12] and [13].

### 3.2 Bank Structure

Figure 3.2 shows the structure of a bank for our proposed DRAM architecture based on HBM2. A single bank consists of multiple subarrays, each of which is further divided into 8 mats sharing the same global word line. With the

---

<sup>1</sup>Reproduced from [17]

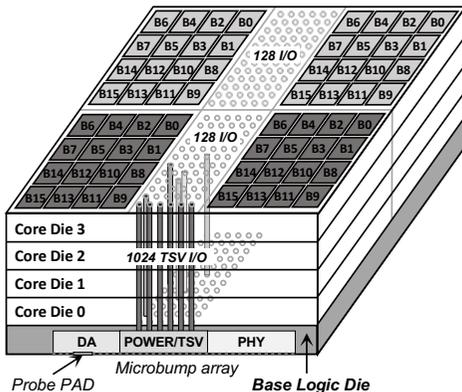


Figure 3.1: Baseline HBM2 architecture<sup>1</sup>

row size of 1KB, activating a single mat reads out 128B of row data, which is a common cacheline size for GPUs. Exploiting this characteristic, we reorganize the column address mapping of mats so that one mat houses a whole 32B column. To enable an activation of a single mat (instead of all eight), we simply add AND gates to the global word line. Such design increases the time to process a READ/WRITE command by 14 memory cycles as it takes 14 extra cycles to burst out a 32B atom through a 16-bit-wide datapath (16 memory cycles in total) instead of a 128-bit-wide datapath (2 memory cycles in total).

To mitigate the effect on READ/WRITE processing time from a narrower path to I/O, we also employ a proposal similar to half-DRAM [13]. The main intuition of the Half-DRAM proposal is that it is possible to utilize two set of bitlines (and helper flip-flops (HFFs)) for activating a single DRAM cell worth of data by making a row decoder drives two half mats (the right half of the mat on the left and the left half of the mat on the right) instead of a single mat. As shown in Figure 3.2, two half mats now utilize two sets of the 16 bitlines and this reduces the READ/WRITE processing time to 8 memory cycles (i.e., 6-cycle

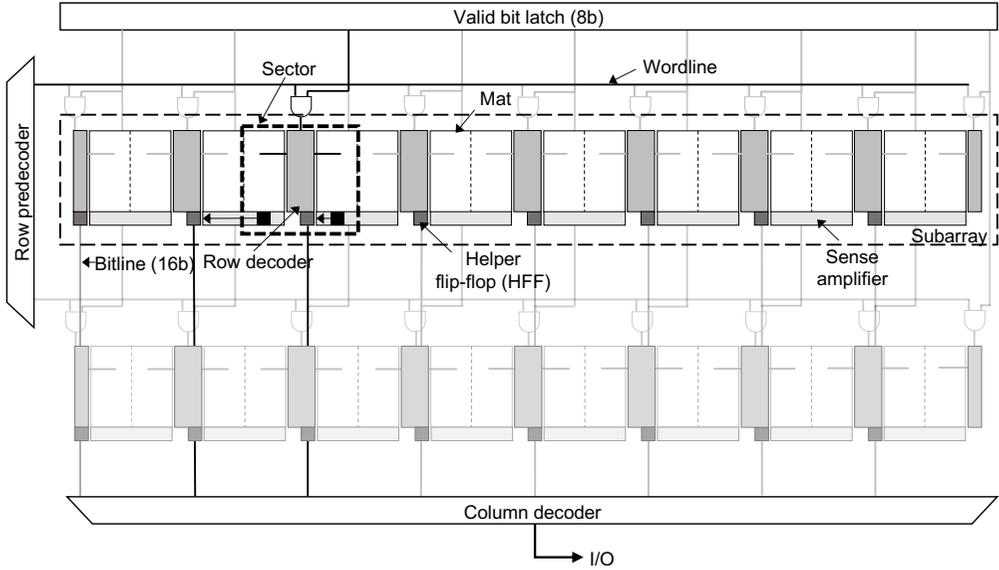


Figure 3.2: Detailed view of PPA bank architecture

increase). Note that we modify column mapping of mats so that a whole column address fits in two corresponding half mats. Throughout the paper, we call these two corresponding half mats a *sector* as shown in Figure 3.2.

To handle this increase in READ/WRITE command processing time, we need to adjust DRAM's timing parameters. First, timing parameter  $\tau_{AA}$ , which represents the time between the read command and the first data output on bus, needs to be increased as the proposed bank structure requires extra cycles to output the data. So  $\tau_{AA}$  is increased by 6 memory cycles.

Figure 3.3 above describes how the  $\tau_{AA}$  timing is lengthened when data being fetched by a cycle-by-cycle waveform. After corresponding *sector* activated, the 16-bit-wide bitlines on both sides are utilized to buffer the requested 32B data. The data is fetched 32 bits per cycle, and it takes 8 cycles to fetch 256 bits. Since the first cycle of fetch data and  $\tau_{AA}$  timing can overlap, and the last fetch and two bursts can overlap, thus it takes a total of 6 cycles to buffer the data

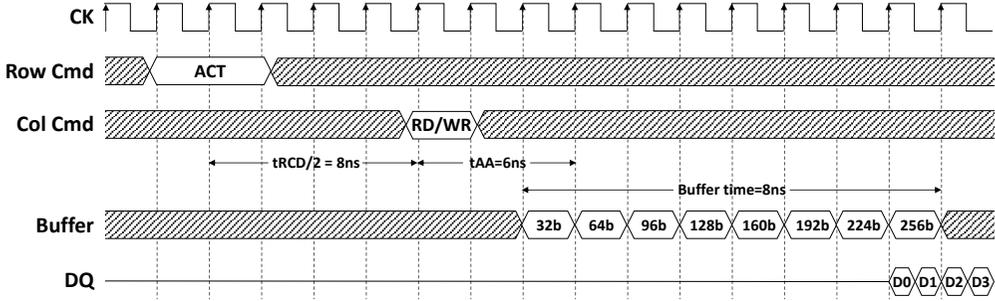


Figure 3.3: Data fetch timing diagram through the narrow bitline

through the narrow bitline.

The timing between column commands to the same bank has to be increased. While a memory controller compliant to HBM standards already has  $t_{CCD}$ , column command to column command delay, we need a variation of this because we only need to increase the delay between column command to column command *to the same bank*. We denote this parameter  $t_{CCD_S}$  and set it to  $t_{CCD}+6$ . This requires a slight timing change to the memory controller. Lastly, other READ/WRITE related delays (e.g.,  $t_{WR}$ ,  $t_{WTR}$ , and  $t_{RTP}$ ) needs to be increased by six cycles as well.

While these mechanisms reduce the peak bank bandwidth by up to  $4\times$  since the time it takes to handle a single READ/WRITE command increases to 8 cycles from 2 cycles. However, this often does not lead to a decrease in overall memory bandwidth since HBM2 specification over-provisions DRAM banks. For example, the evaluated configuration includes 32 banks per channel, where each bank can provide up to 128 bits/cycle. On the other hand, each channel, despite having 32 banks, supply data at 256 bits/cycle. Assuming balanced distributions across 32 banks, each bank only needs to supply 8 bits/cycle to saturate the channel bandwidth. In other words, each bank achieving  $1/16\times$  of its peak throughput is enough to saturate the channel in this case. For this

reason, although our proposed bank structure reduces the peak throughput of a single bank by  $4\times$ , it is unlikely to affect the overall memory throughput, which is often first limited by channel throughput.

### 3.3 Delayed Activation

To specify which *sector* to activate we use delayed activation. When a DRAM device receives **ACTIVATE** commands, the DRAM device decodes row address as usual but does not actually perform an activation and buffer the row address. Instead, the activation happens when a column command arrives. Once a column command (i.e., **READ/WRITE**) arrives, the column address is first decoded and it is used to determine which DRAM *sector* it should activate. Then, a partial activation for that particular *sector* is performed and followed by actual **READ/WRITE** operation. Figure 3.4 shows how this delayed activation scheme affects DRAM timing. First, since **ACTIVATE** does not actually perform an activation,  $\tau_{\text{RCD}}$  becomes shorter (by half according to our estimation using CACTI-3DD [18]). At the same time, since the activation happens in column commands,  $\tau_{\text{AA}}$  (i.e., the timing of read command to the first output data on the bus) and  $\tau_{\text{WL}}$  (i.e., the timing of write command to the first input data on the bus) should be increased by the reduced  $\tau_{\text{RCD}}$  amount. In our configuration,  $\tau_{\text{RCD}}$  is originally set to 16ns and thus  $\tau_{\text{RCD}}$  is reduced by 8ns while  $\tau_{\text{AA}}$  and

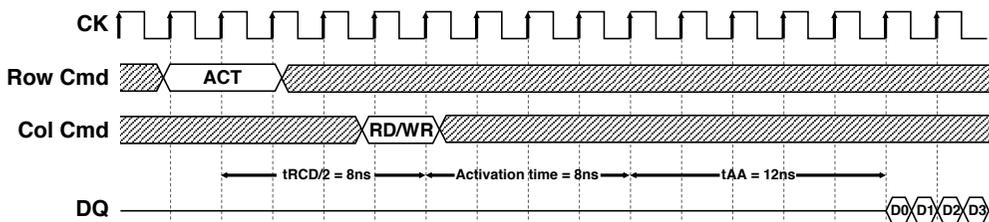


Figure 3.4: Waveform of proposed delayed activation

$\tau_{WL}$  are increased by 8ns. This scheme basically avoids unnecessary activation at the expense of potential 8ns extra latency for `READ` and `WRITE` command. The rationale behind this scheme is that such a minor increase in DRAM latency does not usually affect the performance of the latency-tolerant GPU workloads.

## Chapter 4

# Evaluation

### 4.1 Methodology

We evaluate the proposed scheme using GPGPU-Sim [20]. Table 4.2 shows the configuration we used for the simulation. We assume HBM2 device architecture based on a recent HBM2 design [17, 21] with pseudo-channel mode enabled. We evaluated proposed DRAM architecture based on GTX780-TI device replacing timing model of HBM2 device with existing timing model on DRAM system configuration of the GPGPU-sim, which originally modeled on GDDR5. This GPGPU-sim model coupled with HBM2 is a 1/4 scale down version of the Nvidia P100 [22], a product using HBM2 devices.

We evaluate the performance impact of our scheme across several GPU workloads including memory-intensive general-purpose workloads. We run both popular deep learning workloads on Caffe [23] (augmented with the in-house cuDNN-like library) and several GPU workloads including various memory-intensive workloads from Rodinia [24]. To evaluate energy efficiency, we utilize the GPUWattch [25] integrated with GPGPU-Sim. For DRAM energy parameters, we take numbers from [3]. Lastly, we estimate the area overhead of the proposed scheme using CACTI-3DD [18].

---

<sup>1</sup>GPU architecture parameter from [19]

Platform	Nvidia GTX 780TI <sup>1</sup>
Warp size	32
# of SM cores	16
Execution model	In-order
Max warps per SM	64
Size of register file	256KB (per SM)
# of register banks	24
Warp scheduler	Greedy then oldest
Shared memory	48KB
L1 Cache	16KB
L2 Cache	1536KB

Table 4.1: Platform parameters

DRAM System parameters	
Channel/Device	8
Slices/Device	4-Hi
Banks/Channel	32
Clock frequency	1000MHz
Burst length	4
DQ	×128

Table 4.2: DRAM system parameters

<b>HBM2</b>	<b>1024b @ 1000MHz (ns)</b>
	$t_{RP} = 16, t_{RC} = 45, t_{RAS} = 29, t_{RCD}/2 = 8,$ $t_{CCDS} = 2, t_{CCDL} = 10, t_{RRD} = 2, t_{WR} = 15, t_{CL} = 12$

Table 4.3: HBM2 timing parameters

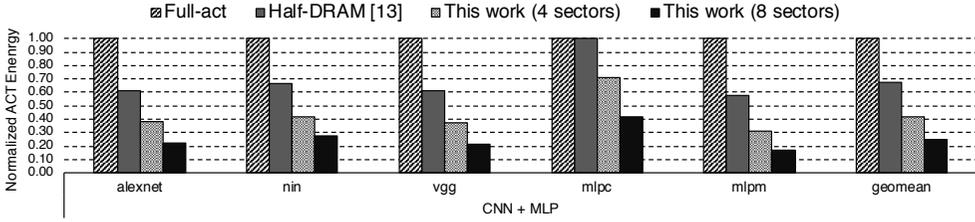


Figure 4.1: Activation energy savings on CNN and MLP workloads

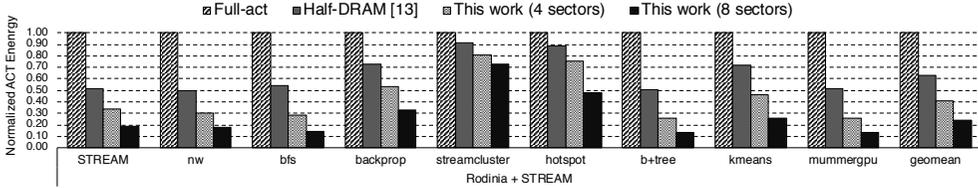


Figure 4.2: Activation energy savings on general workloads (Rodinia and STREAM)

## 4.2 DRAM Energy Savings

Figure 4.1 and 4.1 compare the DRAM activation energy of the baseline full activation, Half-DRAM [13], and our work with 4 and 8 *sectors*. To first order, the activation energy is proportional to the number of columns activated. The activation energy savings are 37%, 59% and 76% on average for Half-DRAM, and our work with 4 and 8 *sectors*, respectively, over the baseline. The energy savings are particularly pronounced for the workloads with frequent row buffer conflicts. In other word, lower spatial locality on a row buffer leads to greater savings of the activation energy. The CNN and MLP workloads have relatively lower row buffer locality to save activation energy about 75% on average for the 8-*sector* configuration. Among Rodinia benchmarks streamcluster and hotspot have smaller savings due to the higher average row buffer locality.

Occasionally, the activation energy savings are affected by row buffer access

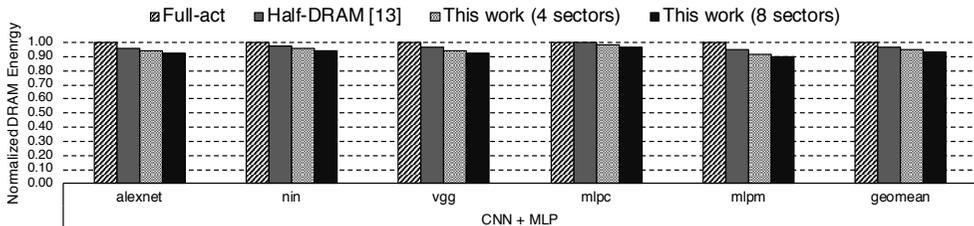


Figure 4.3: DRAM energy savings on CNN and MLP workloads

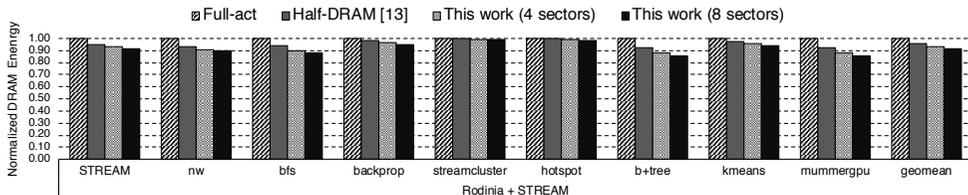


Figure 4.4: DRAM energy savings on general workloads (Rodinia and STREAM)

patterns. For instance, memory accesses in *mlpc* frequently fall on both halves of a row buffer. This leads to little activation energy savings with the Half-DRAM configuration. Figure 4.3 and 4.4 show how the activation energy savings are translated to DRAM-wide energy savings. The *8-sector* configuration achieves 7.6% energy savings on average with maximum savings of 14.1%.

### 4.3 Performance Impact

Figure 4.5 demonstrates that both CNN and MLP workloads are tolerant of increased memory latency. The CNN workloads are known to compute-intensive as convolution layers, which dominates the execution time of a CNN, have a lot of data reuse [7] to have relatively low off-chip memory access rate. Thus, they are able to maintain a high degree of memory-level parallelism and hence IPC. In contrast, MLP workloads, which are composed of fully-connected layers only,

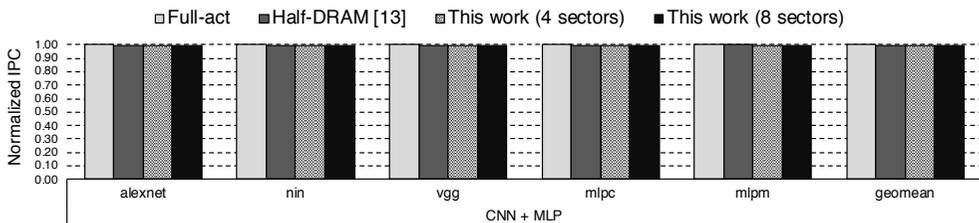


Figure 4.5: Performance degradation on CNN and MLP workloads

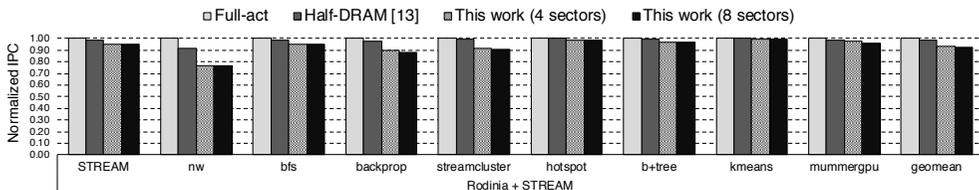


Figure 4.6: Performance degradation on general workloads (Rodinia and STREAM)

are known to be memory-intensive as there is no reuse of weight parameters in these layers. However, compared with recent results from Google’s TPU [7], our MLP workloads are less memory-intensive due to fewer layers and smaller input data sets (Cifar-10 and MNIST). MLP workloads also have a lot of memory-level parallelism and is not sensitive to memory latency. Overall, both CNN and MLP workloads show only negligible IPC degradation.

To evaluate performance impact on non-DNN workloads we take memory-intensive GPU workloads from Rodinia [24] as shown on Figure 4.6. These workloads have a lower degree of memory-level parallelism than DNN workloads. For instance, needleman-wunsch (nw) has a fairly complex control flow with frequent branch divergence, thus suffering up to 22% IPC degradation with the proposed scheme. In contrast, other workloads, such as hotspot, kmeans, and streamcluster, are compute-intensive with a high degree of memory-level

parallelism, thus experiencing less performance hit than the others.

The IPC degradation is attributed to a couple of reasons. First, due to the narrower datapath between a DRAM mat and the I/O, the column access time ( $t_{AA}$ ) is increased substantially. This also negatively affects the latency of a column read/write request directed to the same bank as the previous column request. Second, there is an additional latency cost (8ns in our setup) when a new *sector* needs to be activated in the currently open row. Our proposed DRAM device activates the requested *sector* lazily only when a column request is directed to it. By activating only those *sectors* that are actually read or written, we may have a performance hit for workloads with good spatial locality in DRAM accesses. This problem may be alleviated by increasing the *sector* granularity (e.g., from 8 *sectors* to 4 *sectors* per DRAM row), while losing some of the energy savings with potential overfetching within a *sector*.

## 4.4 Area Overhead

We estimated area overhead incurred by additional circuitry using CACTI-3DD [18]. The area overhead for the portion added to the inside of the dram core includes the following: latches which hold valid bit vector per bank, and 9 AND gates added per subarray. The *sector* selection latch logic is modeled based on the local sense amplifier inside the core, and the NAND gate uses the NAND gate model used in the core. Overall, the die area overhead is 0.3% which we believe acceptable.

## Chapter 5

# Conclusion

This thesis presents a practical partial activation scheme for 3D stacked DRAM with applications to deep learning workloads without significant modifications to the standard HBM2 DRAM interface. To achieve high energy efficiency while maintaining low performance overhead, we exploit the latency tolerance of emerging deep learning workloads to trade DRAM latency for energy efficiency. Consequently, our proposal demonstrates substantial DRAM energy savings with minimal performance hit for both the deep learning workloads and other conventional GPU workloads. This benefit comes with a very low implementation (area) cost and minimal adjustments of DRAM timing parameters over the standard HBM2 DRAM interface.

# Bibliography

- [1] JEDEC, *JEDEC Standard JESD235A: High Bandwidth Memory (HBM) DRAM*. JEDEC Solid State Technology Association, Virginia, USA., 2015.
- [2] Hybrid Memory Cube Consortium, *Hybrid Memory Cube Specification 2.1*, 2015.
- [3] N. Chatterjee, M. O'Connor, D. Lee, D. R. Johnson, S. W. Keckler, M. Rhu, and W. J. Dally, "Architecting an energy-efficient dram system for gpus," in *2017 IEEE International Symposium on High Performance Computer Architecture (HPCA)*, 2017.
- [4] M. O'Connor, N. Chatterjee, D. Lee, J. Wilson, A. Agrawal, S. W. Keckler, and W. J. Dally, "Fine-grained dram: Energy-efficient dram for extreme bandwidth systems," in *Proceedings of the 50th Annual IEEE/ACM International Symposium on Microarchitecture*, 2017.
- [5] E. Cooper-Balis and B. Jacob, "Fine-grained activation for power reduction in dram," *IEEE Micro*, 2010.
- [6] A. N. Udipi, N. Muralimanohar, N. Chatterjee, R. Balasubramonian, A. Davis, and N. P. Jouppi, "Rethinking dram design and organization for energy-constrained multi-cores," in *Proceedings of the 37th Annual International Symposium on Computer Architecture*, 2010.

- [7] N. P. Jouppi *et al.*, “In-datacenter performance analysis of a tensor processing unit,” in *Proceedings of the 44th Annual International Symposium on Computer Architecture*, ISCA ’17, 2017.
- [8] A. Krizhevsky, I. Sutskever, and G. E. Hinton, “Imagenet classification with deep convolutional neural networks,” in *Advances in neural information processing systems*, 2012.
- [9] K. He, X. Zhang, S. Ren, and J. Sun, “Deep residual learning for image recognition,” in *The IEEE Conference on Computer Vision and Pattern Recognition*, CVPR ’16, 2016.
- [10] S. Chetlur, C. Woolley, P. Vandermersch, J. Cohen, J. Tran, B. Catanzaro, and E. Shelhamer, “cudnn: Efficient primitives for deep learning,” 2014.
- [11] Y. Sato *et al.*, “Fast cycle ram (fcram); a 20-ns random row access, pipelined operating dram,” in *1998 Symposium on VLSI Circuits. Digest of Technical Papers*, 1998.
- [12] Y. Lee, H. Kim, S. Hong, and S. Kim, “Partial row activation for low-power dram system,” in *2017 IEEE International Symposium on High Performance Computer Architecture*, HPCA ’17, Feb 2017.
- [13] T. Zhang, K. Chen, C. Xu, G. Sun, T. Wang, and Y. Xie, “Half-dram: A high-bandwidth and low-power dram architecture from the rethinking of fine-grained activation,” in *Proceeding of the 41st Annual International Symposium on Computer Architecture*, ISCA ’14, 2014.
- [14] H. Ha, A. Pedram, S. Richardson, S. Kvatinsky, and M. Horowitz, “Improving energy efficiency of dram by exploiting half page row access,” in *2016*

*49th Annual IEEE/ACM International Symposium on Microarchitecture (MICRO)*, MICRO '16, 2016.

- [15] Y. Kim, V. Seshadri, D. Lee, J. Liu, and O. Mutlu, “A case for exploiting subarray-level parallelism (salp) in dram,” in *2012 39th Annual International Symposium on Computer Architecture (ISCA)*, 2012.
- [16] Micron Technology, Inc, *DDR2 Posted CAS# Additive Latency*, 2003.
- [17] H. Jun, J. Cho, K. Lee, H. Y. Son, K. Kim, H. Jin, and K. Kim, “Hbm (high bandwidth memory) dram technology and architecture,” in *2017 IEEE International Memory Workshop (IMW)*, 2017.
- [18] K. Chen, S. Li, N. Muralimanohar, J. H. Ahn, J. B. Brockman, and N. P. Jouppi, “Cacti-3dd: Architecture-level modeling for 3d die-stacked dram main memory,” in *Proceedings of the Conference on Design, Automation and Test in Europe, DATE '12*, 2012.
- [19] G. Koo, Y. Oh, W. W. Ro, and M. Annavaram, “Access pattern-aware cache management for improving data utilization in gpu,” in *2017 ACM/IEEE 44th Annual International Symposium on Computer Architecture (ISCA)*, ISCA '17, 2017.
- [20] A. Bakhoda, G. L. Yuan, W. W. Fung, H. Wong, and T. M. Aamodt, “Analyzing cuda workloads using a detailed gpu simulator,” in *Performance Analysis of Systems and Software, 2009. ISPASS 2009. IEEE International Symposium on*, IEEE, 2009.
- [21] J. C. Lee and the others, “18.3 a 1.2v 64gb 8-channel 256gb/s hbm dram with peripheral-base-die architecture and small-swing technique on heavy

- load interface,” in *IEEE International Solid-State Circuits Conference (ISSCC)*, 2016.
- [22] NVIDIA, <https://images.nvidia.com/content/tesla/pdf/nvidia-tesla-p100-PCIe-datasheet.pdf>, 2016.
- [23] Y. Jia, E. Shelhamer, J. Donahue, S. Karayev, J. Long, R. Girshick, S. Guadarrama, and T. Darrell, “Caffe: Convolutional architecture for fast feature embedding,” in *Proceedings of the 22nd ACM International Conference on Multimedia, MM '14*, 2014.
- [24] S. Che, M. Boyer, J. Meng, D. Tarjan, J. W. Sheaffer, S. Lee, and K. Skadron, “Rodinia: A benchmark suite for heterogeneous computing,” in *2009 IEEE International Symposium on Workload Characterization (IISWC)*, 2009.
- [25] J. Leng, T. Hetherington, A. ElTantawy, S. Gilani, N. S. Kim, T. M. Aamodt, and V. J. Reddi, “Gpuwattch: Enabling energy optimizations in gpgpus,” in *Proceedings of the 40th Annual International Symposium on Computer Architecture, ISCA '13*, 2013.

## 국문초록

GPU는 심층 학습 애플리케이션을 실행하는 데 널리 사용된다. 오늘날의 high-end GPU는 HBM (High-Bandwidth Memory)과 같은 3D 적층 DRAM 기술을 채택하여 엄청난 대역폭을 제공하므로 많은 전력을 소비한다. GPU에서 수천 개의 동시 스레드가 발생하면 빈번한 row buffer conflict로 인해 상당한 양의 DRAM 에너지가 낭비된다. 이러한 낭비를 줄이기 위해 3D 적층 DRAM에 대한 partial row activation 기법을 제안한다. 풍부한 memory-level parallelism 이 있는 딥 러닝 워크 로드의 latency tolerance를 활용해서, DRAM latency를 지불하고 에너지 절감을 얻을 수 있다. 본 제안에서 딥 러닝 및 기타 기존 GPU 워크 로드에서 성능 저하를 최소화하면서 DRAM activation energy의 상당한 절감 효과를 보여 준다. 본 제안은 매우 낮은 면적 비용으로 표준 HBM2 DRAM 인터페이스에 대한 DRAM 타이밍의 최소한의 변경만으로 구현할 수 있다는 장점이 있다.

**주요어:** CNN, GPU, DRAM 아키텍처, 에너지 효율, HBM2

**학번:** 2017-22393

# Acknowledgements

먼저 제가 학업을 수행할 수 있도록 다방면으로 지원을 아끼지 않으신 존경 하는 부모님 감사드립니다. 부모님이 아니었다면 제가 하는 어떠한 일도 이루어질 수 없었을 것 입니다. 저의 학문과 연구의 길을 밝혀주신 등대와 같은 교수님 존경 하고 감사합니다. 항상 저에게 따끔한 조언 뿐만 아니라 긍정적인 에너지와 계속 연구 할 수 있는 힘을 주셨습니다.

연구실에서 3년이라는 시간동안 동고동락해온 찬노형과 기태형 그리고 성민이 형 으로 구성된 Typed Architecture team과 함께 연구 하면서 많은 것들을 배웠고 그 결과물들을 학회에 제출 할 수 있어서 뜻 깊은 경험이었습니다.

본 연구를 하면서 도움을 주신 분들께 감사를 드립니다. 연구의 디테일 한 부분까지 검토 해주신 함태준 박사님, 학부 인턴임에도 연구에 많은 기여를 한 한성이에게 깊은 감사를 전합니다.

연구실 생활을 하면서 많은 긍정적인 에너지를 공유할 수 있어서 정말 감사 했습니다. 힘들때 술 한잔 기울일 수 있었던 학범이형과 재영이형, 무슨얘기를 하더라도 잘 웃어주고 들어주는 영환이형, 가끔 연구에 지쳤을때, 보드게임을 함께 즐겼던 준이형과 문경이 누나, 뭐든지 물어봐도 거의 모르는게 없는 종현이형, 2년동안 같이 수업도 듣고 연구실 생활의 시작과 끝을 함께한 대연이와 천이, 수학도 잘하고 논리의 끝이 날카로운 성학이, 힘들 때마다 “이겨내야죠” 라고 말해줬던 예진이, 타르트와 쿠키를 잘 만들어왔던 성준이, 회사생활을 함에 있어서 현실적이고 실질적인 조언을 많이 해주신 신이형 석용이형, 행정 업무를 맡아 주시고 발레를 좋아하는 미림누나 연구실 모든 분들 감사드립니다. 마지막으로, 이 논문이 나오는 데 간접적이거나 도움이 된 분들 모두 감사드립니다. 2019년 1월